

# PCCP

Accepted Manuscript



This is an *Accepted Manuscript*, which has been through the Royal Society of Chemistry peer review process and has been accepted for publication.

*Accepted Manuscripts* are published online shortly after acceptance, before technical editing, formatting and proof reading. Using this free service, authors can make their results available to the community, in citable form, before we publish the edited article. We will replace this *Accepted Manuscript* with the edited and formatted *Advance Article* as soon as it is available.

You can find more information about *Accepted Manuscripts* in the [Information for Authors](#).

Please note that technical editing may introduce minor changes to the text and/or graphics, which may alter content. The journal's standard [Terms & Conditions](#) and the [Ethical guidelines](#) still apply. In no event shall the Royal Society of Chemistry be held responsible for any errors or omissions in this *Accepted Manuscript* or any consequences arising from the use of any information it contains.

## Hydrophobic effects within the dynamic pH response of polybasic tertiary amine methacrylate brushes

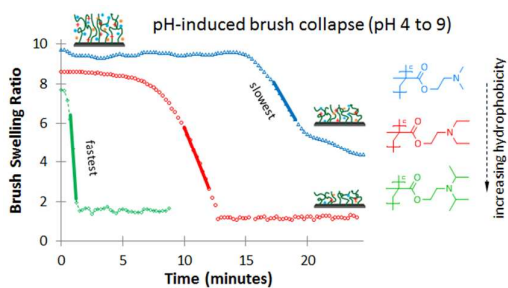
Joshua D. Willott,<sup>a</sup> Ben A. Humphreys,<sup>a</sup> Timothy J. Murdoch,<sup>a</sup> Steve Edmondson,<sup>b</sup> Grant B. Webber,<sup>a</sup> Erica J. Wanless,<sup>\*a</sup>

<sup>a</sup> Priority Research Centre for Advanced Particle Processing and Transport, University of Newcastle, Callaghan, NSW 2308, Australia

<sup>b</sup> School of Materials, University of Manchester, Oxford Road, Manchester, M13, 9PL, United Kingdom

\* corresponding author: [erica.wanless@newcastle.edu.au](mailto:erica.wanless@newcastle.edu.au)

### TOC entry



Monomer hydrophobicity dominates the kinetics of the pH response of tertiary amine methacrylate brushes as determined by *in situ* ellipsometry and QCM-D kinetic and equilibrium measurements.

**Abstract**

The solvation and swelling behaviour of three dialkylaminoethyl methacrylate polymer brushes, of varying hydrophobicity, have been investigated using a combination of *in situ* ellipsometry and a quartz crystal microbalance with dissipation (QCM-D). At low pH the tertiary amine groups of the three polymers are protonated and all three brushes are significantly solvated and swell by adopting an extended conformation. As the pH is increased the weak polybasic brushes become increasingly deprotonated and collapse via solvent expulsion. By employing high temporal resolution measurements we have found that monomer hydrophobicity has a direct influence on the dynamics of this pH-response. The most hydrophobic poly(2-diisopropylamino)ethyl methacrylate (poly(DPA)) brush exhibits the fastest maximum swelling rate. This maximum swelling rate is reduced with decreasing monomer hydrophobicity for the 2-diethylamino, and even further for the 2-dimethylamino analogues. For all three brushes, the corresponding collapse transition is slower and compounded by an induction time that decreases with monomer hydrophobicity. Here also, the maximum collapse rate is greatest for the most hydrophobic polymer. This domination of the pH-response kinetics by monomer hydrophobicity is attributed to attractive hydrophobic forces between polymer segments overcoming the repulsive electrostatic forces between the tertiary amine residues.

## Introduction

During recent decades so-called intelligent materials prepared by grafting responsive polymer brushes from interfaces have received considerable attention.<sup>1,2</sup> Polymer brushes are formed by anchoring polymer chains to a surface by one end at a high enough grafting density that they are forced to extend normal to the grafting interface. Grafted polyelectrolytes, specifically weak polybases, represent one such class of smart surfaces. Their physicochemical properties like degree of solvation,<sup>3</sup> wettability<sup>4</sup> and lubricity<sup>5</sup> can be controlled by a range of environmental stimuli including pH, ionic strength and temperature. By appropriate choice of monomer, researchers have utilised the properties of polyelectrolyte brushes to develop, for example, tuneable friction,<sup>6</sup> superoleophobic,<sup>7,8</sup> as well as anti-fouling surfaces.<sup>9,10</sup>

The behaviour of polyelectrolyte brushes is governed by several factors, including excluded volume interactions, electrostatic interactions (mainly repulsion between charged monomer units) and osmotic pressure imparted by the absorption of solvent and counterions. The latter two of these factors are affected by the ionic strength of the overlying solution. However, unlike strong polyelectrolyte brushes whose monomer units are charged under all conditions, weak polyelectrolyte brushes are composed of ionisable monomer groups. Consequently weak polyelectrolyte brushes exhibit an overall charge density that depends on the pH and ionic strength of the local solution making them pH-responsive.<sup>11</sup>

For weak polybases, the brush becomes charged at pH values below the brush  $pK_a$  due to protonation of the monomer groups. This charging process causes the brush to swell due to the increased Coulombic repulsion between chains and the associated osmotic pressure rise that occurs as a result of ingress of solvent and counterions into the brush.<sup>12,13</sup> With increasing pH, moving towards and then above the  $pK_a$ , the brush deprotonates and becomes progressively more uncharged. In this reverse process, neutralisation of the charged groups causes the brush to collapse as the decreased inter- and intra-chain electrostatic repulsions become dominated by the hydrophobic polymer segment interactions and water and counterions are expelled from within.

One class of weak polybasic polymer brushes are those formed using tertiary amine methacrylate monomers. Of this family the most commonly studied are poly(2-dimethylamino)ethyl methacrylate (poly(DMA)) brushes which display classical pH responsive behaviour with an apparent  $pK_a$  value in the vicinity of physiological pH.<sup>14-16</sup> These brushes have been shown to exhibit pH controllable interfacial lubrication,<sup>5</sup> wettability<sup>17,18</sup> and molecular transport,<sup>19</sup> as well as being used in combination with other polymers for the development of antimicrobial and infection-resistant

surfaces.<sup>20, 21</sup> The less studied and more hydrophobic poly(2-diethylamino)ethyl methacrylate (poly(DEA))<sup>13, 22-26</sup> and poly(2-diisopropylamino)ethyl methacrylate (poly(DPA))<sup>4, 22, 27</sup> analogues of poly(DMA) also display pH sensitive behaviour. Owing to their increased hydrophobicity, untethered poly(DEA) and poly(DPA) homopolymers have been shown to exhibit pH dependent solubility, being insoluble at neutral and basic pH at room temperature.<sup>28, 29</sup> In contrast, the less hydrophobic poly(DMA) is water-soluble in acidic, neutral and basic media (up to pH 11) at room temperature.<sup>29</sup><sup>30</sup> When incorporated into end-tethered brushes it is expected that this hydrophilic/hydrophobic balance coupled with the inherent confinement of the polymer chains will significantly influence brush charging and solvation as has been reported recently for a family of weak polyacids.<sup>31</sup>

Formally, the  $pK_a$  value for a weak polybase is defined as the pH at which half of the basic monomer groups are associated with a proton. However, in comparison to small-molecule bases (and acids), polybases (and polyacids) exhibit a broader range of solution pH over which protons are exchanged. Thus more commonly an apparent  $pK_a$  value, or pH range, is used to describe the pH at which the polymer transitions from a charged to an uncharged state. Untethered poly(DEA) has a similar apparent  $pK_a$  value to poly(DMA), 7.3 and 7.0, respectively,<sup>28</sup> however, poly(DEA) is more hydrophobic.<sup>29</sup> The apparent  $pK_a$  of untethered poly(DPA) is considerably lower at 6.0 and is substantially more hydrophobic.<sup>28, 29</sup> Significantly for brushes, the apparent  $pK_a$  transition is broader still and may be shifted, since the protonation equilibrium of the tertiary amine groups (for polybases) is strongly influenced by the inherent confinement of the polymer chains.<sup>13, 32</sup>

While the equilibrium pH-response of individual polybasic brushes has received considered attention,<sup>3, 5, 13-15, 22, 25</sup> herein we present a comprehensive comparative study of the dynamic behaviour of three polybasic tertiary amine methacrylates. Our previous studies have focussed on poly(DEA) brushes grown from both particulate and planar substrates where we have demonstrated highly reversible equilibrium behaviour (charge state, brush thickness and viscoelastic nature) within the pH range of 4 and 9.<sup>3, 12, 13</sup> We have also reported on the real-time swelling and collapse of poly(DEA) brushes where the collapse transition was considerably slower (~8 times) than the converse rapid swelling transition.<sup>13</sup> In this previous work we postulated that the collapse process was significantly hindered due to the formation of region of denser partially desolvated polymer (a skin) which acts as a diffusion barrier to the egress of protons, water and counterions from within the brush. To further explore this hypothesis, in the current work we have investigated the equilibrium and dynamic behaviour of the pH-response of three polybasic brushes with varying hydrophobicity; poly(DMA), poly(DEA) and poly(DPA). Using high temporal resolution *in situ* ellipsometry and quartz crystal microbalance with dissipation monitoring (QCM-D) we have

developed insight into the role of hydrophobicity on brush dynamics. We will demonstrate that invoking a dense layer at the periphery of the brush is indeed not necessary to explain the movement of solvent and counterions during the collapse transitions.

## Experimental

The chemical structures of the three polymers studied are shown in Figure 1. The increased pendant alkyl group length and steric bulk around the tertiary amine group mean that the polymers increase in hydrophobicity from poly(DMA) through to poly(DPA).

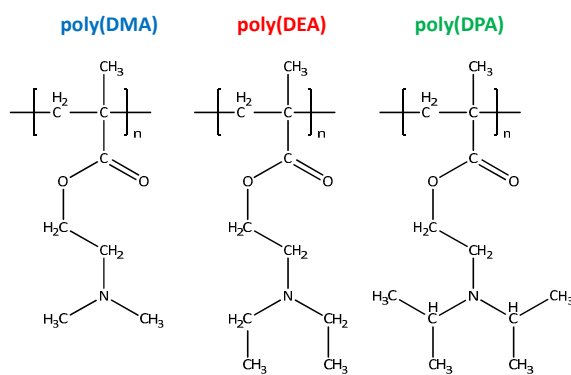


**Figure 1.** The chemical structures of poly(2-dimethylamino)ethyl methacrylate (poly(DMA)), poly(2-diethylamino)ethyl methacrylate (poly(DEA)) and poly(2-diisopropylamino)ethyl methacrylate (poly(DPA)).

### Materials and Chemicals

Silicon wafers were purchased from Silicon Valley Microelectronics, Santa Clara, California, USA. Quartz crystal microbalance sensors (QSX 303, ~4.95 MHz fundamental resonant frequency) with 50 nm silica coating were purchased from Q-Sense, Sweden. Silane-initiator functionalisation reagents including (3-aminopropyl)triethoxysilane, tetrahydrofuran, triethylamine and 2-bromoisobutyryl bromide were purchased from Sigma Aldrich and used as received. The tetrahydrofuran and triethylamine were dried over 4 Å molecular sieves (ARCOS Organics) before use (for at least 1 day). The inhibitor was removed from 2-(dimethylamino)ethyl methacrylate (DMA), 2-(diethylamino)ethyl methacrylate (DEA) and 2-(diisopropylamino)ethyl methacrylate (DPA) monomers, all purchased from Sigma Aldrich, by gravity feeding through a 10 cm length and 2 cm diameter alumina column (activated, basic). Inhibitor was removed from the monomer immediately before polymerisation. Polymerisation reagents copper(II) bromide (99.999%), 2,2'-bipyridine (≥99%), L-ascorbic acid

( $\geq 99\%$ ), and (+)-sodium L-ascorbate ( $\geq 98\%$ ) were purchased from Sigma Aldrich and used as received. Methanol (99.8%, anhydrous, Sigma Aldrich) and isopropyl alcohol (99.7%, Chem-Supply Pty Ltd) were used as solvents in the polymerisations. All aqueous *in situ* ellipsometry and QCM-D measurements were performed in the presence of 10 mM potassium nitrate (Asia Pacific Specialty Chemicals Ltd  $>99\%$ ) electrolyte. Solution pH values were accurate to  $\pm 0.1$  pH unit and adjustments were made by adding a minimum amount of 0.01 M or 0.1 M nitric acid (RCI Labscan Ltd) or potassium hydroxide (AR grade, Chem-Supply Pty Ltd) to a feed reservoir of electrolyte solution which was subsequently flowed into the sample chamber through air-impermeable silicone tubing and peristaltic pump. Milli-Q water (18.2 M $\Omega$  at 25 °C, Millipore) was used to prepare all solutions.

#### *Wafer and QCM sensor initiator functionalisation*

Cleaned wafers and QCM sensors (see ESI<sup>†</sup>) were amine-functionalised by exposure to (3-aminopropyl)triethoxysilane (APTES) vapour at  $< 5$  mbar for 30 min at room temperature before being annealed in air at 110 °C.<sup>13, 22</sup> The surfaces were then bromine-functionalised by immersing them in a solution of 2-bromoisobutryl bromide (0.26 mL) and anhydrous triethylamine (0.3 mL) in anhydrous tetrahydrofuran (10 mL) under a nitrogen atmosphere for 60 min.<sup>13</sup> The surfaces were then removed and rinsed with tetrahydrofuran, ethanol and Milli-Q water and dried under a stream of nitrogen.

#### *Brush polymerisation via ARGET ATRP*

The poly(DMA), poly(DEA) and poly(DPA) brushes were synthesised from the bromine-initiator moieties, by the 'grafting from' method, using activators continuously regenerated by electron transfer atom transfer radical polymerisation (ARGET ATRP) methodology.<sup>12, 13</sup> A typical brush polymerisation was carried out in either methanol (for DMA and DEA) or isopropyl alcohol: water (9:1 v/v, for DPA) at  $22 \pm 0.5$  °C using an ARGET ATRP recipe consisting of monomer/catalyst/ligand/reducing agent in a molar ratio of 2500/1/10/10. Here the catalyst used was copper(II) bromide, the ligand was 2,2'-bipyridine and the reducing agent was either sodium ascorbate (for DMA and DEA) or ascorbic acid (for DPA). The ratio of monomer to solvent was 50:50 v/v. For more detailed brush synthesis protocol please see the ESI<sup>†</sup>.

Previous studies have demonstrated that the ideal dry thickness for the brushes to be investigated by ellipsometry is  $\sim 20$  nm.<sup>3, 13</sup> As such the poly(DMA) and poly(DEA) brushes were synthesised for 30 min while the poly(DPA) brush was synthesised for 60 min with measured brush thickness values given in Table 1. For the QCM-D measurements similar dry thickness brushes were used for poly(DEA) and poly(DPA). For poly(DMA), a brush of comparable dry thickness was initially studied

but displayed changes in resonant frequency and dissipation that indicated a loss of coupling between the brush and solvent had occurred. This was attributed to the high degree of solvation of the poly(DMA) brush which was subsequently confirmed by ellipsometry. Similar behaviour has been observed previously.<sup>33,34</sup> Consequently a thinner poly(DMA) brush was synthesised and studied using QCM-D as listed in Table 1.

#### *Ellipsometry studies*

A Nanofilm EP3 single wavelength imaging ellipsometer with a 532 nm wavelength laser running EP3View software was used, with the ellipsometric parameters ( $\Psi$  and  $\Delta$ ) modelled using the WVASE32 software with details given in the ESI†. The dry brush thickness values are shown in Table 1.

**Table 1.** Dry brush thickness values for the poly(DMA), poly(DEA) and poly(DPA) brushes studied.

	Ellipsometric Brush Thickness (nm)	
	Ellipsometry Studies	QCM-D Studies <sup>a</sup>
Poly(DMA)	23.4±0.7	13.9±0.2
Poly(DEA)	18.0±0.2	22.5±0.7
Poly(DPA)	21.1±0.3	23.6±0.2

<sup>a</sup> measured for brushes grown on sister wafers (see ESI†)

*In situ* ellipsometric measurements were performed on the brush-modified wafers within a Nanofilm SL fluid cell with optical glass windows at a laser beam angle of incidence of 60°. Only a single angle of incidence was available as the beam must be perpendicular to the cell windows. The cell had a trapezoidal geometry with an internal volume of 0.70 mL with an exposed sample area of 10 mm × 18 mm. All wet measurements were performed in 10 mM potassium nitrate electrolyte maintained at the desired pH value at 21 ± 1.0 °C.

The experiments were conducted under a constant flow of electrolyte solution at ~4.3 mL·min<sup>-1</sup>. This flow rate was selected to ensure rapid change of the desired pH inside the fluid cell (with a tubing plus cell fluid residence time of ~10 s and ~30 s to switch the pH from 9 to 4 and ~40 s for pH 4 to 9 for pH switching kinetic experiments).<sup>3</sup> The flow was also selected in order to work in a constant supply regime where the pH value inside the cell is maintained at the desired level by controlling the pH value of the external electrolyte reservoir.<sup>3</sup> For equilibrium brush measurements the solution flow and pH were maintained over timescales of at least 25 min until a steady state was achieved. For overnight storage between measurements, the fluid cell was left filled with 10 mM potassium

electrolyte at ambient pH (~5.5) with the pump turned off. Each brush was maintained in an aqueous environment for the duration of all experiments.

The ellipsometric quantities  $\psi$  and  $\Delta$  were recorded by employing a 'kinetic' script that performed repeated nulling one-zone measurements every 15 s. Each  $\psi$  and  $\Delta$  pair were modelled to determine the solvated (wet) brush thickness using a multilayer-slab model (for more details please see the ESI†). A measured  $\Delta$  offset of  $-1.5^\circ$  due to fluid cell window effects on the measurement of  $\Delta$  was accounted for in the optical model.<sup>35</sup>

#### *Static contact angle measurements*

Contact angle measurements were performed using an OCA15 dynamic contact angle instrument (DataPhysics, Germany). Brushes of each polymer were immersed in aqueous electrolyte in an inverted orientation. A captive air bubble was placed on the surface and the left- and right-hand contact angle recorded. Reported values are the average of measurements of three separate bubbles for each condition. The solution pH was adjusted as required *in situ* such that the surface remained immersed throughout.

#### *QCM-D studies*

A KSV Z500 quartz crystal microbalance with dissipation monitoring capabilities (QCM-D, KSV, Finland) was used, with the sensor (~5 MHz, Q-Sense, Sweden) housed in a parallel flow chamber sealed with an o-ring and glass window. The cell had a cylindrical geometry with an internal cell volume of 0.25 mL with a circular exposed sample area of 14 mm diameter. QCM-D operates by measuring changes in the frequency ( $\Delta f$ ) and energy dissipation ( $\Delta D$ ) of the shear oscillatory motion of a piezoelectric quartz sensor upon changes in the mass coupled to the sensor vibration. This makes the technique sensitive to changes in the solvent retained within or hydrodynamically coupled to polymer brushes.<sup>36</sup> Oscillations of the QCM sensor at the fundamental resonant frequency (~5 MHz) and higher overtones (~15, ~25, ~35 and ~45 MHz) were measured with frequency ( $\Delta f_n/n$ ) and dissipation ( $\Delta D_n$ ) data for the 3<sup>rd</sup> ( $n = 3$ ) overtone (~15 MHz) presented in this study.

One of the challenges facing the use of QCM-D when studying solvated polymer brushes is separating the frequency response from changes in mass and viscoelasticity associated with the brush. For sufficiently rigid films that behave elastically, generally when the absolute value of  $\Delta D_n/(\Delta f_n/n) < 0.4 \times 10^{-6} \text{ Hz}^{-1}$ ,<sup>37</sup> the Sauerbrey equation can be used to extract the areal mass density of the film<sup>38</sup> (known as the Sauerbrey or acoustic mass) which includes a contribution due to the mass of solvent entrained within and coupled with the film. However in this study, as is the case for

most soft dissipative films, the above criterion is not met and the application of the Sauerbrey model is no longer applicable. As such we report the recorded changes in resonant frequency as a measure of brush solvation instead of calculating a mass change associated with the brush response.

As with the *in situ* ellipsometry measurements, all QCM-D measurements were conducted at a constant flow rate ( $\sim 4.3 \text{ mL}\cdot\text{min}^{-1}$ ) of 10 mM potassium nitrate electrolyte solution at the desired pH. At this flow rate, the fluid cell residence time was  $\sim 3.5 \text{ s}$  with  $< 15 \text{ s}$  for pH change from 9 to 4 and vice versa. This high flow rate was not found to have any impact on the frequency response of the sensors due to the parallel flow geometry of the cell. For equilibrium brush measurements the solution flow and pH were maintained over timescales of at least 25 min until a steady state was achieved. All experiments were conducted at a controlled temperature of  $21 \pm 0.2 \text{ }^\circ\text{C}$ . For overnight storage the flow chamber was left filled with 10 mM potassium nitrate solution at ambient pH ( $\sim 5.5$ ) with the pump switched off. Each brush was left solvated over the entire duration of the experiments.

## Results and Discussion

All measurements were made in 10 mM background potassium nitrate electrolyte so that any changes in ionic strength due to the pH adjustments were negligible compared to the overall solution ionic strength. Furthermore, since the charge and swelling behaviour of weak polybasic brushes is considerably affected by ionic strength, 10 mM was selected because the brushes will exist in the 'salted-brush' regime where the ionic strength inside the brush is a maximum and is essentially equal to the ionic strength of the bulk solution (see for example Zhulina and Borisov, and Nap *et al.* and references therein).<sup>39,40</sup> At this ionic strength brush thickness is expected to be maximised for a given pH value for the brushes studied.<sup>13</sup>

### *Equilibrium brush pH-response*

Figure 2 shows the equilibrium contact angles of the three brushes as the overlying solution pH was cycled between 9 and 4. These data clearly shows the poly(DMA) brush is the most hydrophilic at both pH 9 and 4, the poly(DEA) brush is more hydrophobic and the poly(DPA) brush the most hydrophobic. This is a result of the increased alkyl group length and substitution around the tertiary amine group (see Figure 1). It is also evident in the reversibility of the data in Figure 2 that the brushes remain stable to changes in solution pH, i.e. there is no degradation of the brush. Table 2 presents the difference between the contact angles measured at pH 9 and 4 for all brushes. It is clear

from both Figure 2 and Table 2 that the difference in the nature of the brushes between the two solvent conditions increases with hydrophobicity.

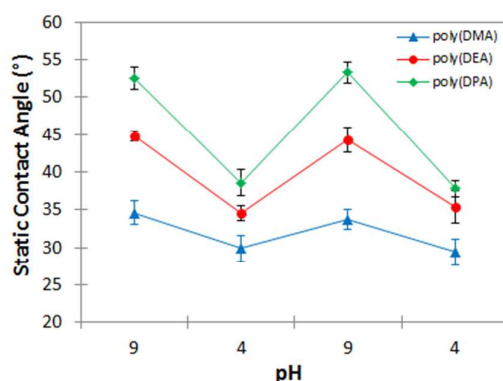


**Figure 2.** Static contact angles at pH 9 and 4 for the three brushes immersed in 10 mM potassium nitrate electrolyte.

**Table 2.** Difference between the pH 9 and 4 static contact angles for the poly(DMA), poly(DEA) and poly(DPA) brushes.

	pH 9 Contact Angle (°)	pH 4 Contact Angle (°)	Difference Between pH 9 and pH 4 Contact Angle (°)
poly(DMA)	34.8 ± 0.6	27.5 ± 0.3	7.3 ± 0.7
poly(DEA)	44.5 ± 0.4	35.0 ± 0.6	9.5 ± 0.7
poly(DPA)	53.0 ± 0.5	38.2 ± 0.5	14.8 ± 0.7

Figure 3 shows the equilibrium swelling ratio (ratio of wet to dry brush thickness) as a function of solution pH for the three polybasic brushes as measured by *in situ* ellipsometry. Swelling ratio is a useful way to compare how much solvent is incorporated into the brush at any given solution condition and removes the dependence on the dry brush thickness. In these experiments the initial solution was pH 9, the pH was incrementally reduced then returned to 9. At low pH values the brushes exist in their most swollen conformation represented by a high swelling ratio which confirms a high grafting density. The high swelling at low pH is expected since the tertiary amine groups of the polymers are protonated causing water and counterions to be absorbed by the brush. At low pH, the poly(DMA) brush has the highest degree of solvation (largest swelling ratio) with the poly(DEA) brush swollen by less solvent and the poly(DPA) brush containing the least. This trend in the swelling ratio of the three brushes at low pH is supported by the static contact angle measurements, Figure 2, and is a result of brush hydrophobicity. Such dependency of equilibrium

brush conformation on polymer hydrophobicity has recently been demonstrated for a family of weak polyacids by Lu *et al.*<sup>31</sup>

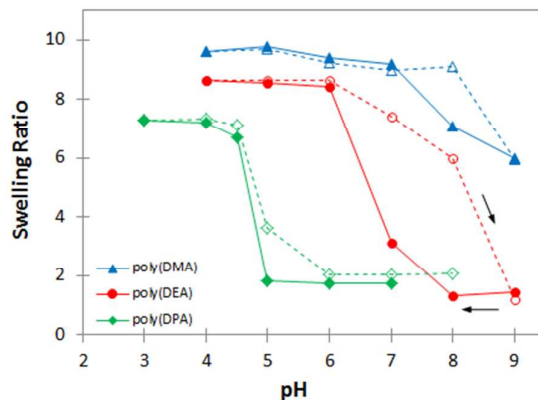


**Figure 3.** Ellipsometric pH-response of poly(DMA) ( $\blacktriangle$ ), poly(DEA) ( $\bullet$ ) and poly(DPA) ( $\blacklozenge$ ) brushes as a function of pH in 10 mM  $\text{KNO}_3$  background electrolyte. Swelling ratio is the ratio of the solvated to dry brush thickness. The solid lines represent the brush swelling transition and the dashed lines correspond to the subsequent collapse of the brush. The arrows indicate the experiment chronology starting from pH 9.

A striking feature of Figure 3 is the broad pH-range over which the brushes move from a collapsed conformation (less swollen) to more swollen conformation as the pH is decreased, and vice versa as the pH is raised. This gradual solvent uptake as the pH is lowered contrasts with the sharper  $\text{pK}_a$  transition behaviour associated with untethered polybases<sup>28</sup> and is in accord with our previous measurements of poly(DEA) brushes.<sup>3, 13, 22</sup> The apparent  $\text{pK}_a$  of the poly(DPA) brush is shifted to a considerably lower pH value compared to the other two polymers which is attributed to the greater hydrophobicity and hence lower solubility of poly(DPA). This is in line with the behaviour of untethered poly(DPA) in aqueous solution.<sup>28, 29</sup> It is notable that the swelling transition for the most hydrophilic poly(DMA) brush occurs at an even higher pH than that of the poly(DEA) brush, and is also higher than the  $\text{pK}_a$  ( $\sim$ pH 7.0) reported for untethered poly(DMA).<sup>28</sup> This behaviour is somewhat unexpected, however, due to the convolution of the measured polymer chain solvation with the inferred protonation equilibrium, which together yield a broad transition pH, and thus make it impossible to pinpoint an actual  $\text{pK}_a$  value. Moreover, it has been observed that the pH range over which untethered poly(DMA) dissociates protons is much broader than either poly(DEA) or poly(DPA).<sup>28</sup>

Upon increasing the pH above the apparent  $pK_a$  the brushes collapse by solvent expulsion as the tertiary amine groups are gradually deprotonated. At pH 9, well-above the  $pK_a$  of the brushes, the brushes are uncharged and hydrophobic, though they are still expected to have a degree of water associated with them.<sup>22, 41</sup> The collapse process is hysteretic in nature, when compared to the swelling transition, with a higher pH value required to collapse the brush. The hysteresis between the swelling and collapse processes is most pronounced in the case of the poly(DEA) brush as previously reported.<sup>13, 25</sup> This hysteric behaviour is further explored later when the kinetics of the brush swelling and collapse transitions is considered. It is also evident from Figure 3 that the two more hydrophobic brushes, poly(DEA) and poly(DPA), collapse significantly more than the poly(DMA) brush. This is in accord with the behaviour of the untethered polymers, where poly(DMA) remains water-soluble at neutral and basic pH whereas the two more hydrophobic polymers aggregate at pH values at and above their  $pK_a$ .<sup>28-30</sup> This difference in hydrophobicity also accounts for the range of pH over which the brush conformational changes occur shifting toward basic values from poly(DPA) to poly(DMA).

QCM-D measurements were also performed to further investigate the equilibrium behaviour of the three polybasic brushes as a function of solution pH. QCM-D is an established technique able to monitor the behaviour of polyelectrolyte brushes.<sup>3, 36, 42-44</sup> QCM-D measurements are used here to provide complementary insight into the solvation of the brushes and energy transfer between the oscillating sensor/brush and the solvent. A decrease in  $\Delta f$  (more negative value) corresponds to an increase in the amount of material coupled to the motion of the crystal; conversely a more positive value represents a loss of coupled material. Here, this represents a change in the amount of solvent entrained by the brush because the mass of polymer is invariant.  $\Delta D$  is a measure of how rapidly the motion of the sensor is damped by the brush and is typically used as an indicator of the chain extension, separation and also viscoelasticity of the brush layer. Energy dissipation by polymer brushes is significantly influenced by the behaviour of the tails of polymer at the periphery of the brush. A lower magnitude of  $\Delta D$  represents polymer chains interacting less with the solvent which leads to a more rigid film, while the opposite is true for a greater magnitude of  $\Delta D$  which corresponds to a more viscous film.

The frequency and dissipation changes for the three polybasic brushes are presented in Figure 4. In a standard QCM-D experiment the zero for both frequency and dissipation would represent the bare sensor, so that any adsorbed amount may subsequently be determined. This is not possible here where the polymer brush is grown in an external environment to the instrument. Instead, we have chosen zero  $\Delta f$  and  $\Delta D$  to correspond to the equilibrium response at pH 4, and so the behaviour of

the brush can be interpreted in comparison to this state. The data plotted is for the 3<sup>rd</sup> overtone, *i.e.*  $\Delta f_3/3$  and  $\Delta D_3$ . The frequency data in Figure 4a emulates the general trends of the ellipsometry data in Figure 2. For all three brushes as the pH is incrementally decreased to pH 4 the measured  $\Delta f$  value decreases while simultaneously  $\Delta D$  (Figure 4b) increases. This corresponds to the brushes adopting a more extended conformation (from  $\Delta D$ ), with more solvent entrained inside the brush coupled to the oscillatory motion of the brushes/solvent with the QCM sensor (from  $\Delta f$ ). The magnitude of change in frequency for the poly(DMA) brush from its uncharged (pH 9) to charged state (pH 4) is smaller compared to the other more hydrophobic brushes. This confirms that the poly(DMA) is more solvated when uncharged compared to the more hydrophobic brushes, in line with Figure 3. Furthermore, as observed in the ellipsometry data, the poly(DEA) and poly(DPA) brushes exhibit a history-dependent response, in both the  $\Delta f$  and  $\Delta D$  values, between the swelling and collapse transitions. For the poly(DMA) brush there is minimal hysteresis in the QCM-D data compared to both ellipsometric measurements and to the other two polymers recorded with QCM-D. To further elucidate these behaviours the kinetics during brush swelling and collapse were explored, see later discussion. Figure 4 shows the broad range over which the three brushes swell and collapse in the QCM-D data signalling that the charging and discharging of the brushes and hence their solvation, is a gradual process which occurs over several pH units. What is notable here is that the poly(DMA) brush responds over a much broader pH range than the corresponding ellipsometry data. This is not overly surprising since QCM-D is much more sensitive to subtle changes in brush solvation and conformation than ellipsometry which measures overall brush thickness and therefore can be regarded as an ensemble average over the measured area.

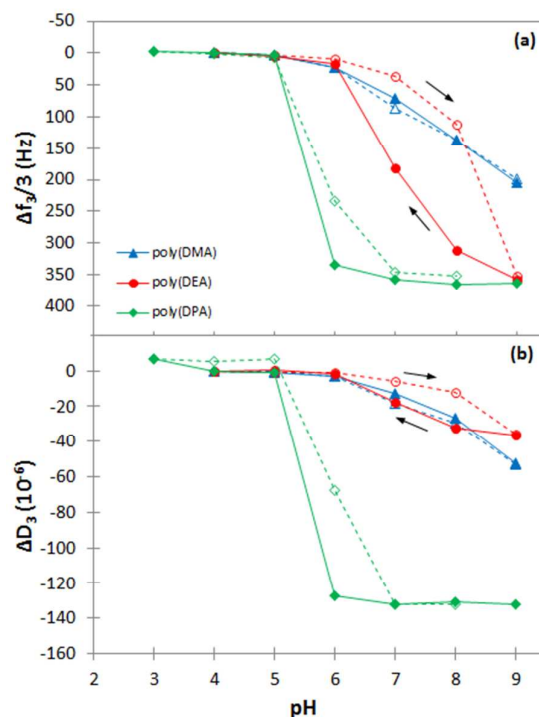


**Figure 4.** Change in (a) QCM-D frequency ( $\Delta f_3/3$ ) and (b) dissipation response ( $\Delta D_3$ ), normalised to the equilibrium pH 4 value, as the pH was incrementally acidified (solid lines) and then returned to pH 9 (dashed lines) for the three polybasic brushes studied, poly(DMA) ( $\blacktriangle$ ), poly(DEA) ( $\bullet$ ) and poly(DPA) ( $\blacklozenge$ ). The arrows indicate the experiment chronology starting from pH 9.

Figure 4b presents the change in dissipation values for the three brushes. At high pH the poly(DMA), poly(DEA) and poly(DPA) brushes dissipate less energy compared to their pH 4 state indicating that the brushes adopt a more rigid, collapsed conformation compared to the more viscous, extended brushes at low pH values. What is apparent is the large change in dissipation for the poly(DPA) brush between pH 4 and 9. Looking at this massive change in dissipation in isolation from the frequency data suggests that the poly(DPA) brush is significantly more desolvated than the other two brushes consistent with the local environment measured for the uncharged untethered homopolymers in solution.<sup>29</sup> However, the change in  $\Delta f$  is very similar for the poly(DEA) and poly(DPA) brushes, *i.e.* similar change in solvation which suggests that the  $\Delta D$  data for poly(DPA) tells us something else. The ellipsometry data, Figure 3 also indicate that the swelling ratio of the poly(DEA) and poly(DPA) brushes are similar at pH values above their  $pK_a$ . The magnitude of the dissipation value measured by the QCM-D is a combination of two possible damping mechanisms; between the brush and the solvent and within the brush itself. So here the QCM-D data indicates that the extent of damping

within the brush itself is different for poly(DEA) and poly(DPA) between low and high pH states. That is, the difference in the energy dissipation of the collapsed and swollen states of the poly(DPA) brush is greater than the poly(DEA) brush. We postulate that this difference is due to the branched nature of the DPA monomer which creates greater internal steric stresses within the brush. It may also be possible there is a difference in brush grafting density, however, based on the work of Sudre *et al.*<sup>45</sup> we estimate from our swelling ratios that the difference could be at most 15% which is insufficient to fully explain the observed differences in the dissipation data

By plotting  $\Delta D$  as a function of  $\Delta f$ , information concerning the conformational changes occurring within the three brushes during the swelling and collapse processes can be obtained. Since  $\Delta f$  is a measure of the solvation and desolvation of the brush and  $\Delta D$  measures the energy dissipated due to the brush conformation (*i.e.* chain extension), the relationship between the two quantities can be used to describe the cooperativity between the solvation and conformation changes in polymer films.<sup>46-48</sup> Figure 5 presents the frequency and dissipation responses for the poly(DMA), poly(DEA) and poly(DPA) brushes in the pH-range 9-4 for both the swelling and collapse transitions in the form of a  $\Delta D$ - $\Delta f$  plot.

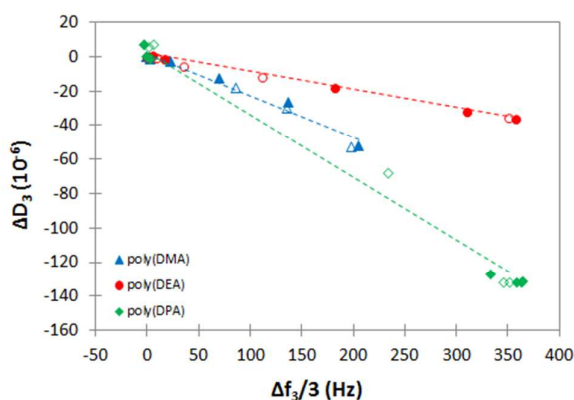


**Figure 5.** Change in dissipation ( $\Delta D_3$ ) versus change in frequency ( $\Delta f_3/3$ ) response in the pH range 9-4 for the poly(DMA) (▲), poly(DEA) (●) and poly(DPA) (◆) brushes studied. Both dissipation and frequency are normalised to the pH 4 value for each brush. The dashed lines indicate the linear relationship between  $\Delta D$  and  $\Delta f$  for each brush. The filled and open symbols are the data from Figure 3 collected as the pH is increased and decreased, respectively.

As is clear in Figure 5,  $\Delta D$  increases with decreasing  $\Delta f$ , for all three brushes, indicating the solvation of grafted chains and swelling of the brushes upon decreasing pH. While for the collapse process the opposite is true, with  $\Delta D$  decreasing with increasing  $\Delta f$  indicative of the desolvation of the grafted

chains accompanied by the collapse of the brushes at increasing pH values. What is striking for each of the three brushes is that there is a single linear relationship between  $\Delta f$  and  $\Delta D$  for both the swelling and collapse transitions. This indicates that there is a single process associated with swelling and collapse for each brush. Specifically, the solvation, protonation and swelling (chain extension) occur simultaneously, and the desolvation and deprotonation is concurrent with the chain collapse. However, the varied gradients of these relationships confirm that the precise nature of these processes is different when the monomer is varied.

#### *Time-resolved pH-induced swelling and collapse*

Following the equilibrium experiments, the kinetics of the swelling and collapse transitions was investigated by switching the pH directly between 9 and 4 using both *in situ* ellipsometry and QCM-D. Our previous work has shown the rates of poly(DEA) brush response (swelling and collapse) are dependent on the solution flow rate when a low flow rate is used; predominantly at flow rates less than  $\sim 1.6 \text{ mL}\cdot\text{min}^{-1}$ .<sup>3</sup> This is because the brush behaviour becomes limited by transport of protons, hydroxides, and/or counterions and does not indicate intrinsic brush behaviour. Therefore a constant high flow rate was adopted ( $\sim 4.3 \text{ mL}\cdot\text{min}^{-1}$ ) so that any changes in the dynamic behaviour of the brushes could be attributed to inherent brush behaviour and not the experimental design. The pH response of all three brushes was robust with several highly reproducible pH cycles between pH 9 and 4 performed.

When interpreting the pH switching response of the three brushes one must first consider the hydrophobicity of the polymers themselves,<sup>28, 29</sup> which dictates the difference in relative hydrophobicity of the brushes in pH 9 and pH 4 electrolyte solution. As the least hydrophobic polymer, poly(DMA) exhibits the smallest hydrophobicity difference between the uncharged pH 9 brush and the charged pH 4 brush. Poly(DPA) is the most hydrophobic and thus the hydrophobicity difference between uncharged and charged state is greatest for poly(DPA). Poly(DEA) exhibits intermediate behaviour. This behaviour is confirmed by static contact angle measurements (captive bubble beneath inverted brush surface) for the three brushes immersed in pH controlled 10 mM potassium nitrate electrolyte as presented in Figure 2 and Table 2. Where poly(DMA) is the most hydrophilic brush at both pH 9 and 4, as expected, with poly(DEA) more hydrophobic and poly(DPA) the most hydrophobic. *In situ* ellipsometry and QCM-D kinetic measurements reveal that for all three brushes the swelling transition, pH 9 to 4, was rapid with significant swelling of the brush occurring within 3 minutes (see Figure S1a and S1b, ESI<sup>†</sup>). It is also evident that measurable swelling occurs within the timeframe of complete solution exchange for both the ellipsometer and QCM-D measurement cells. This is akin to the swelling of other poly(DEA) brushes<sup>3, 13</sup> as well as an adsorbed

poly(DEA) microgel film.<sup>49</sup> The swelling process is rapid as there is a considerable osmotic driving force for solvent to move into the partially dehydrated brushes as they become protonated at low pH. However, when studying the maximum swelling rates for the three brushes a clear trend between the three brushes emerges, see Table 3. Poly(DMA) has the lowest maximum swelling rates measured by ellipsometry and QCM-D, while the rates for poly(DEA) swelling are higher and the rates for poly(DPA) the highest. This behaviour may be expected from the relative hydrophobicity difference between the uncharged and charged states of the polymers. When the pH is changed from pH 9 to pH 4 the brushes are protonated at the periphery, become more hydrophilic and begin to swell via the uptake of water and counterions; the opposite is true when the pH is changed from 4 to 9 where the brushes are uncharged and more hydrophobic. The key point to make from Table 2 is that the difference in contact angle between pH 9 and 4 increases in magnitude from poly(DMA) through to poly(DPA). This means that poly(DPA) has the largest hydrophobicity difference between the two states. As such there is a pronounced driving force for solvent to move into this brush upon protonation. This driving force is weaker in the case of poly(DEA) and poly(DMA).

**Table 3.** Maximum brush swelling and collapse from *in situ* ellipsometry and QCM-D kinetic measurements as well as the induction times until brush collapse from the ellipsometry kinetics.

	<i>In Situ</i> Ellipsometry				Induction Time to Brush Collapse	QCM-D		
	Maximum Swelling and Collapse Rates					min	Maximum Solvation (swelling) and Desolvation (collapse) Rates	
	Swelling min <sup>-1</sup> *	nm/min	Collapse min <sup>-1</sup> *	nm/min			Solvation Δf·min <sup>-1</sup>	Desolvation Δf·min <sup>-1</sup>
Poly(DMA)	2.8	67	-1.1	-24	~14	-251	55	
Poly(DEA)	5.0	89	-1.5	-29	~7	-482	86	
Poly(DPA)	11.3	238	-9.6	-181	n/a	-1090	112	

\*Change in swelling ratio per unit time.

Both the *in situ* ellipsometry and QCM-D data are consistent with a rapid, single step swelling process which slows upon reaching equilibrium. We propose a cooperative process by which the periphery of the brush is protonated first resulting in the solvation and swelling of the brush which allows deeper penetration of solvent and counterions into the brush until it reaches maximum solvation and swelling, as illustrated in Figure 6a. There is also a difference in the entropy gain upon solvation for the three brushes. For example the greater steric stress within the poly(DPA) brush (due to the branching on the tertiary amine) will provide a greater entropic driving force for brush swelling. It should be reiterated here that the kinetic experiments are performed under high flow

rates where the flux of protons to the swelling brush is essentially constant. As protons are depleted from the overlying solution near the brush they are constantly renewed; the observed differences in maximum swelling rate are therefore attributed to intrinsic brush behaviour.

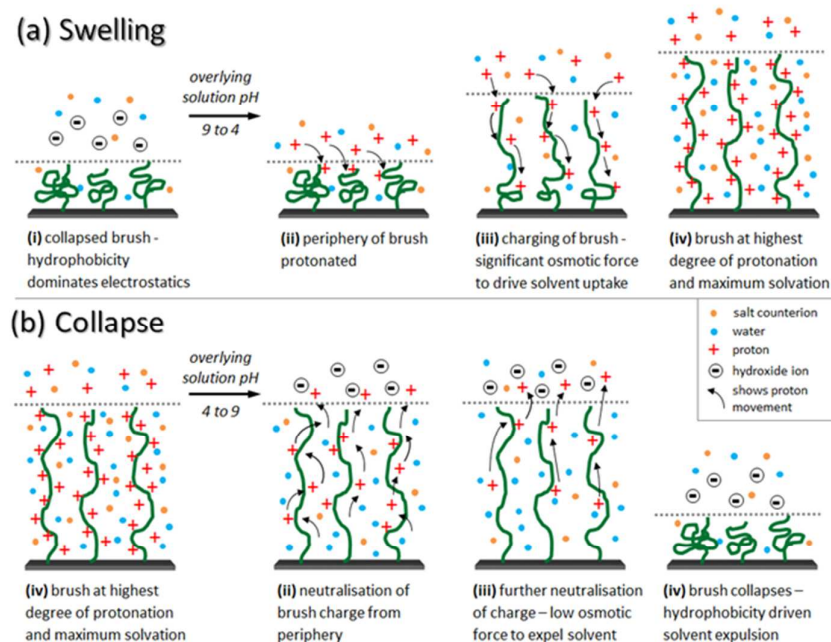


**Figure 6.** Schematic representations of the proposed mechanisms responsible for the (a) brush swelling and (b) brush collapse transitions.

*In situ* ellipsometry data for the collapse of each brush as the pH was switched from pH 4 to pH 9 is presented in Figure 7. For the poly(DMA) and poly(DEA) brushes, the collapse transition is considerably slower than the respective swelling transition (see Figure S1a), with significant induction times of  $\sim 14$  and  $\sim 7$  min, respectively, before the brush collapse is initiated. The induction time is measured as the time taken from the new solution reaching the inside of the cell to the initial decrease in the swelling ratio from the plateau value. It is perhaps not unexpected that brush collapse is slower than the swelling transition as there is a lower osmotic driving force; at pH 4 the brush is well-solvated, while at pH 9 the brush is poorly-solvated compared to the overlying solution. The expulsion of water from the brush is instead driven by the changing hydrophobicity of the polymer brush during collapse. In our previous work solely detailing the behaviour of poly(DEA) brushes, we proposed that a denser region of partially desolvated polymer forms upon deprotonation of the inherently hydrophobic brush upon exposure to pH 9 solution.<sup>13</sup> This was believed to be responsible for the lengthy induction time prior to collapse. However, in this broader

work it can now be demonstrated that the overall polymer hydrophobicity and hence solubility is the key to understanding this brush response, and that invoking a dense layer at the periphery of the brush is not necessary to explain the movement of solvent and counterions during the collapse transitions.

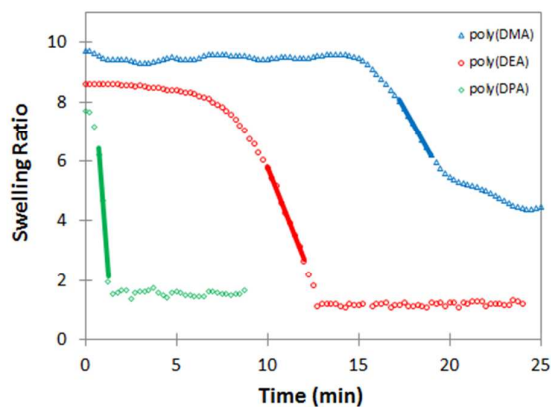


**Figure 7.** Poly(DMA) ( $\Delta$ ), poly(DEA) ( $\circ$ ) and poly(DPA) ( $\diamond$ ) swelling ratio as a function of time upon change in pH from 4 to 9, as measured by *in situ* ellipsometry. Including maximum collapse rates calculated from the data marked with the solid lines. Time zero represents the time at which pH 9 electrolyte solution enters the fluid cell. Once the pH 9 electrolyte reaches the cell there is a mixing period of  $\sim 40$  s before the cell pH changes to pH 9.

With focus on the brush collapse shown in Figure 6b, when the pH is switched from 4 to 9, the peripheral tertiary amine groups are initially deprotonated. This allows for labile tertiary amine protons to relocate from other tertiary amine groups within the brush to occupy the recently vacated ionisable sites. Here, as the brush is gradually neutralised, the overall charge density of the brush decreases as protons within the brush relocate into more electrostatically favourable locations *i.e.* to tertiary amine residues that are further from neighbouring charged residues. This deprotonation process continues until a given degree of charge within the brush is reached as dictated by the polymer hydrophobicity, and the brush collapses. As polymer hydrophobicity increases the entire brush becomes insoluble at a higher degree of charge since the electrostatic repulsion between protonated tertiary amine residues becomes dominated by the increasing favourable polymer-polymer interactions.<sup>50</sup>

The pH-dependent solubility and charging of untethered poly(DMA), poly(DEA) and poly(DPA) homopolymers were demonstrated by Bütün *et al.*<sup>28</sup> They observed that poly(DEA) and poly(DPA) become insoluble at basic pH while poly(DMA) remained soluble up to pH 11 at room temperature.

When acidic aqueous solutions of the homopolymers, with equivalent concentration of ionisable groups based on tertiary amine residues, were titrated against potassium hydroxide, differences in the bulk solution pH response were evident based on polymer hydrophobicity. For poly(DPA), it can be concluded that the homopolymer became insoluble when the solution reached  $\sim$ pH 6. Further addition of potassium hydroxide did not change the solution pH as all added hydroxide ions were neutralised by protons dissociating from the now insoluble polymer. Poly(DEA) exhibited a slow change in pH between 6 and 7 indicating a degree of proton dissociation while the polymer remained soluble. When the pH reached  $\sim$ 7.5 the poly(DEA) became insoluble, and again all extra added hydroxide ions were neutralised by protons released from the polymer. Thus the plots of pH versus added potassium hydroxide for poly(DEA) and poly(DPA) both show a near-horizontal region where the pH is essentially buffered by the discharging of the polymer. Poly(DMA), on the other hand, exhibits a much smoother transition. Between pH  $\sim$ 6 and  $\sim$ 10 the poly(DMA) is observed to slowly deprotonate with added potassium hydroxide, and the poly(DMA) remains soluble throughout. The brush kinetics shown in Figure 7 can be interpreted with respect to this bulk homopolymer behaviour.

The experimental approach of driving the brush collapse through a rapid large rise in pH to above the apparent  $pK_a$  means the relative gradient for deprotonation is steepest for poly(DPA) and weakest for poly(DMA). This is manifest in the observed trend in collapse kinetics reported in Figure 7. For poly(DPA) the collapse is rapid with no apparent induction time. This is attributed to the insolubility of poly(DPA) above pH 6 – 6.5 which results in a rapid phase separation to a rigid film as supported by the QCM-D equilibrium data in Figure 4. Here as the local pH approaches and goes beyond the brush  $pK_a$  the increased hydrophobic interactions between the polymer chains dominate the repulsive electrostatic forces and brush collapses. The poly(DPA) brush does not exhibit an induction time because it can collapse at a higher degree of charge than the other two brushes due to its increased hydrophobicity, as observed with untethered poly(DPA)<sup>28</sup> and predicted by Monte Carlo simulations of untethered weak hydrophobic polyelectrolytes.<sup>50</sup> Again, the experimental design allows for rapid and constant transport of protons out of the brush and facilitates the rapid brush response.

From Table 3 and Figure 7, it is clear that the collapse of poly(DEA) is considerably slower than that of poly(DPA), with a longer induction time and a lower maximum collapse rate as recorded by both experimental methods. The collapse of poly(DMA) is slower again with yet a longer induction time and lower maximum collapse rate. Once more this can be understood by taking into account the hydrophobicity difference between the charged and uncharged brushes. The poly(DEA) brush is less

hydrophobic than the poly(DPA) brush and has a distinctly greater apparent  $pK_a$ . This lower hydrophobicity of poly(DEA) means that the brush needs to be discharged more before the hydrophobic interactions can dominate over the electrostatic repulsion between chains and the brush can start to collapse.<sup>28</sup> Poly(DMA) is soluble in both states and is therefore subject to a lower hydrophobic driving force for collapse. This is manifested in the much slower collapse kinetics compared to the other two brushes. This is in addition to the equilibrium ellipsometry and QCM-D measurements that indicate that the pH required to promote brush collapse, the apparent  $pK_a$ , was highest for poly(DMA). Note also the differences in the shape of the data in Figure 7. For both poly(DPA) and poly(DEA) the swelling ratio decreases at its maximum rate then, within one data point (~15 s), establishes a plateau value for the collapsed state. The poly(DMA) exhibits a more sigmoidal shape in the collapse data where the swelling ratio continues to decrease for many minutes after the maximum collapse rate was observed. This is concordant with insolubility of the poly(DPA) and poly(DEA) brushes and the retention of solubility of the collapsed poly(DMA) brush. Indeed, there is remarkable similarity in the form of our brush data in Figure 7 and the pH titration data for the three untethered homopolymers reported by Bütün *et al.*<sup>28</sup>

## Conclusions

By employing a combination of *in situ* ellipsometry and QCM-D, we have investigated the equilibrium and kinetic pH response of a family of tertiary amine methacrylate brushes. The three polymer brushes have different inherent hydrophobicity and consequently they exhibit diverse pH responsive behaviour in terms of the solvation and desolvation of the brushes during their corresponding swelling and collapse transitions. The most hydrophobic poly(DPA) brush undergoes rapid swelling and collapse (with the highest maximum swelling and collapse rates) upon pH switching between pH 9 and 4. At high pH the brush is uncharged and collapses due to the hydrophobicity of the polymer while at low pH the brush is charged and solvated. The increasingly more hydrophilic poly(DEA) and poly(DMA) brushes display analogous polybasic behaviour in terms of their pH response, however, they both undergo considerably slower brush collapse transitions. We propose a mechanism by which the solvent expulsion and hence brush collapse is directly influenced by polymer hydrophobicity and thus solubility. Here as the polymer hydrophobicity increases, the brush collapses at a faster rate since the repulsive electrostatic forces between charged tertiary amine residues are dominated by favourable polymer segment hydrophobic attractive forces. Poly(DPA) undergoes rapid collapse due to its significantly increased hydrophobicity which is more akin to an overall phase separation.

## Acknowledgements

This research is supported by the Australian Research Council (DP110100041). Undergraduate research student Clinton Daines is thanked for performing the *in situ* contact angle measurements.

†Electronic Supplementary Information (ESI) available: wafer and QCM sensor preparation, brush polymerisation details, ellipsometric measurements, data fitting protocol and optical model, as well as brush swelling kinetics.

## References

1. M. A. Cohen Stuart, W. T. S. Huck, J. Genzer, M. Muller, C. Ober, M. Stamm, G. B. Sukhorukov, I. Szleifer, V. V. Tsukruk, M. Urban, F. Winnik, S. Zauscher, I. Luzinov and S. Minko, *Nat. Mater.*, 2010, **9**, 101-113.
2. O. Azzaroni, *J. Polym. Sci., Part A: Polym. Chem.*, 2012, **50**, 3225-3258.
3. B. T. Cheesman, E. G. Smith, T. J. Murdoch, C. Guibert, G. B. Webber, S. Edmondson and E. J. Wanless, *Phys. Chem. Chem. Phys.*, 2013, **15**, 14502-14510.
4. E. Stratakis, A. Mateescu, M. Barberoglou, M. Vamvakaki, C. Fotakis and S. H. Anastasiadis, *Chem. Commun.*, 2010, **46**, 4136-4138.
5. N. Nordgren and M. W. Rutland, *Nano Lett.*, 2009, **9**, 2984-2990.
6. Q. Wei, M. Cai, F. Zhou and W. Liu, *Macromolecules*, 2013, **46**, 9368-9379.
7. G. J. Dunderdale, C. Urata, D. F. Miranda and A. Hozumi, *ACS Appl. Mater. Interfaces*, 2014, **6**, 11864-11868.
8. G. J. Dunderdale, C. Urata and A. Hozumi, *Langmuir*, 2014, **30**, 13438-13446.
9. M. Kobayashi, Y. Terayama, H. Yamaguchi, M. Terada, D. Murakami, K. Ishihara and A. Takahara, *Langmuir*, 2012, **28**, 7212-7222.
10. W. J. Yang, K.-G. Neoh, E.-T. Kang, S. L.-M. Teo and D. Rittschof, *Prog. Polym. Sci.*, 2014, **39**, 1017-1042.
11. M. Ballauff and O. Borisov, *Curr. Opin. Colloid Interface Sci.*, 2006, **11**, 316-323.
12. B. T. Cheesman, J. D. Willott, G. B. Webber, S. Edmondson and E. J. Wanless, *ACS Macro Lett.*, 2012, **1**, 1161-1165.
13. J. D. Willott, T. J. Murdoch, B. A. Humphreys, S. Edmondson, G. B. Webber and E. J. Wanless, *Langmuir*, 2014, **30**, 1827-1836.
14. S. Sanjuan, P. Perrin, N. Pantoustier and Y. Tran, *Langmuir*, 2007, **23**, 5769-5778.
15. M. Moglianetti, J. R. P. Webster, S. Edmondson, S. P. Armes and S. Titmuss, *Langmuir*, 2010, **26**, 12684-12689.
16. H. Jia, A. Wildes and S. Titmuss, *Macromolecules*, 2012, **45**, 305-312.
17. Q. Zhang, F. Xia, T. Sun, W. Song, T. Zhao, M. Liu and L. Jiang, *Chem. Commun.*, 2008, 1199-1201.
18. A. Zengin, G. Karakose and T. Caykara, *Eur. Polym. J.*, 2013, **49**, 3350-3358.
19. O. Schepelina and I. Zharov, *Langmuir*, 2008, **24**, 14188-14194.

20. L.-A. B. Rawlinson, S. a. M. Ryan, G. Mantovani, J. A. Syrett, D. M. Haddleton and D. J. Brayden, *Biomacromolecules*, 2009, **11**, 443-453.
21. N. Hadjesfandiari, K. Yu, Y. Mei and J. N. Kizhakkedathu, *J. Mater. Chem. B*, 2014, **2**, 4968-4978.
22. L. A. Fielding, S. Edmondson and S. P. Armes, *J. Mater. Chem.*, 2011, **21**, 11773-11780.
23. X. Wang, G. Liu and G. Zhang, *Langmuir*, 2011, **27**, 9895-9901.
24. S. Kumar, X. Tong, Y. L. Dory, M. Lepage and Y. Zhao, *Chem. Commun.*, 2013, **49**, 90-92.
25. P. D. Topham, A. Glidle, D. T. W. Toolan, M. P. Weir, M. W. A. Skoda, R. Barker and J. R. Howse, *Langmuir*, 2013, **29**, 6068-6076.
26. G. J. Dunderdale and J. P. A. Fairclough, *Langmuir*, 2013, **29**, 3628-3635.
27. W. Sun, S. Zhou, B. You and L. Wu, *Macromolecules*, 2013, **46**, 7018-7026.
28. V. Bütün, S. P. Armes and N. C. Billingham, *Polymer*, 2001, **42**, 5993-6008.
29. T. Thavanesan, C. Herbert and F. A. Plamper, *Langmuir*, 2014, **30**, 5609-5619.
30. D. Fournier, R. Hoogenboom, H. M. L. Thijs, R. M. Paulus and U. S. Schubert, *Macromolecules*, 2007, **40**, 915-920.
31. Y. Lu, A. Zhuk, L. Xu, X. Liang, E. Kharlampieva and S. A. Sukhishvili, *Soft Matter*, 2013, **9**, 5464-5472.
32. R. Nap, P. Gong and I. Szleifer, *J. Polym. Sci., Part B: Polym. Phys.*, 2006, **44**, 2638-2662.
33. N. Ishida and S. Biggs, *Macromolecules*, 2007, **40**, 9045-9052.
34. G. Dunér, E. Thormann and A. Dédinaite, *J. Colloid Interface Sci.*, 2013, **408**, 229-234.
35. K. B. Rodenhausen, T. Kasputis, A. K. Pannier, J. Y. Gerasimov, R. Y. Lai, M. Solinsky, T. E. Tiwald, H. Wang, A. Sarkar, T. Hofmann, N. Ianno and M. Schubert, *Rev. Sci. Instrum.*, 2011, **82**, 103111.
36. S. E. Moya and J. Irigoyen, *J. Polym. Sci., Part B: Polym. Phys.*, 2013, **51**, 1068-1072.
37. I. Reviakine, D. Johannsmann and R. P. Richter, *Anal. Chem.*, 2011, **83**, 8838-8848.
38. G. Sauerbrey, *J. Physik*, 1959, **155**, 206-212.
39. E. B. Zhulina and O. V. Borisov, *Langmuir*, 2011, **27**, 10615-10633.
40. R. Nap, M. Tagliazucchi and I. Szleifer, *J. Chem. Phys.*, 2014, **140**, 024910.
41. S. Rauch, P. Uhlmann and K.-J. Eichhorn, *Anal. Bioanal. Chem.*, 2013, **405**, 9061-9069.
42. N. Schüwer and H.-A. Klok, *Langmuir*, 2011, **27**, 4789-4796.
43. P. C. Nalam, L. Daikhin, R. M. Espinosa-Marzal, J. Clasohm, M. Urbakh and N. D. Spencer, *J. Phys. Chem. C*, 2013, **117**, 4533-4543.
44. X. Chu, J. Yang, G. Liu and J. Zhao, *Soft Matter*, 2014, **10**, 5568-5578.
45. G. Sudre, D. Hourdet, C. Creton, F. Cousin and Y. Tran, *Macromol. Chem. Phys.*, 2013, **214**, 2882-2890.
46. F. Höök, M. Rodahl, P. Brzezinski and B. Kasemo, *Langmuir*, 1998, **14**, 729-734.
47. Y. Hou, G. Liu, Y. Wu and G. Zhang, *Phys. Chem. Chem. Phys.*, 2011, **13**, 2880-2886.
48. T. Wang, Y. Long, L. Liu, X. Wang, V. S. J. Craig, G. Zhang and G. Liu, *Langmuir*, 2014, **30**, 12850-12859.
49. S. C. Howard, V. S. J. Craig, P. A. FitzGerald and E. J. Wanless, *Langmuir*, 2010, **26**, 14615-14623.
50. S. Ulrich, A. Laguerre and S. Stoll, *J. Chem. Phys.*, 2005, **122**, 094911.